

Computational study of Th⁴⁺ and Np⁴⁺ hydration and hydrolysis of Th⁴⁺ from first principles

Davi H. T. Amador¹ · Julio R. Sambrano² · Ricardo Gargano³ · Luiz Guilherme M. de Macedo^{1,3}

Received: 19 November 2016 / Accepted: 23 January 2017 / Published online: 14 February 2017
© Springer-Verlag Berlin Heidelberg 2017

Abstract The aqueous solvation of Th and Np in the IV oxidation state was examined using cluster models generated by Monte Carlo simulations and density functional theory embedded within the COSMO continuum model to approximate the effect of bulk water. Our results suggest that the coordination number (CN) for both Th(IV) and Np(IV) should be 9, in accordance to some experimental and theoretical results from the literature. The structural values for average oxygen–metal distances are within 0.01 Å compared to experimental data, and also within the experimental error. The calculated ΔG_{Sol}^0 are in very good agreement with experimental reported values, with deviations at CN = 9 lower than 1% for both Th(IV) and Np(IV). The hydrolysis constants are also in very good agreement with experimental values. Finally, our methodology has the advantage of using a GGA functional (BP86) that not only makes the calculations more affordable computationally than hybrid functional or ab initio molecular dynamics simulations (Car-Parrinello) calculations, but also opens the perspective to use resolution of identity (RI) calculations for more extended systems.

Keywords Actinides in solution · Relativistic effects · DFT · Free energy of solvation of ions · Theoretical hydrolysis constants

Introduction

Despite the environmental [1], political and energetic [2] importance of actinides, the basic characteristics, such as ionization potential and thermodynamic properties for several ions, of many actinides are still unknown, due mainly to experimental difficulties related to their high radioactivity and instability. Furthermore, their chemical behavior is quite complex since they have a large number of oxidation states, and by the appearance of valence 5f orbitals, which are more extended and less shielded by the outer 6s and 6p, making them more prone to participate in bonding than 4f orbitals [3].

It is important to note that understanding the behavior of actinides in aqueous solution is important to the separation and long-term storage of nuclear waste. In particular, studies are still needed on actinides (IV) such as Neptunium and Thorium [4, 5]: Np is considered to be the most problematic actinide [6] due to its high solubility and mobility, whereas the main interest in Th lies in its potential as a source of nuclear fuel [7].

The experimental study of the aqueous chemistry of Th(IV) and Np(IV) requires knowledge of their hydrolysis, which is very complex for Th(IV) due to colloid or polymeric species even at low concentrations [8–10], and for Np [11, 12] due to complex redox, solubility and sorption behavior to hydrologic processes. Since both Np(IV) and Th(IV) are strongly hydrated due to their high charge to ionic radius ratio, elucidation of their aqueous hydration environment is necessary to understand their aqueous chemistry.

This paper belongs to Topical Collection VI Symposium on Electronic Structure and Molecular Dynamics – VI SeedMol

✉ Luiz Guilherme M. de Macedo
lgm@ufpa.br

¹ Faculdade de Biotecnologia, Instituto de Ciências Biológicas, Universidade Federal do Pará (UFPA), Belém, PA 66075-110, Brazil

² Departamento de Matemática, Universidade Estadual Paulista (UNESP), PO Box 473, Bauru, SP 17030-360, Brazil

³ Instituto de Física, Universidade de Brasília (UnB), PO Box 04455, Brasília, DF 70919-970, Brazil

Nevertheless, there is huge experimental uncertainty regarding the number of water molecules present in the first hydration shell (i.e., the coordination number) for Th(IV) and Np(IV), and also for the hydrolysis constants of Th(IV): the coordination numbers (CN) of Np(IV) and Th(IV) have been studied by X-ray experiments, and were estimated to be 8–11 for Th(IV) [13–16] and 8–12 for Np(IV) [11–18], while theoretical calculations suggest 9–10 [19–21] for Th(IV) and 8–9 [22, 23] for Np(IV). In turn, the hydrolysis constants for Th(IV) varies significantly in the literature [9], sometimes more than three orders of magnitude, and, to the best of our knowledge, there is no relativistic density functional calculations for hydrolysis constants of Th(IV).

First principles theoretical calculations are an alternative means of obtaining structural, thermodynamic and chemical properties of actinide ions in the condensed phase [24–26]. In this work, we investigate the structural properties of the hydration shell and thermodynamics of solvated Np(IV) and Th(IV) ions by first principles in order to address preferred CN, molecular structure, binding energies and Gibbs free energies of solvation. The aim was to obtain results at affordable computational costs using a GGA functional, pseudopotentials, cluster-continuum models and metropolis algorithm to generate initial structures.

Computational details

It was necessary to obtain good starting geometries for the clusters before performing the quantum chemical calculations, and these geometries were obtained through Monte Carlo (MC) simulations. The MC simulations were performed using standard procedures [27] for the Metropolis sampling technique in the isothermal-isobaric NpT ensemble. All simulations were performed using the program DICE [28]. In both simulations, the Th⁴⁺ and Np⁴⁺ ions were surrounded by 1000 water molecules at a pressure of 1 atm and temperature of 298 K. After a long equilibration of 1×10^8 steps, the MC simulations were performed with 2×10^8 steps.

In MC simulations, molecules interact via Lennard-Jones (LJ) potential. The LJ parameters [20, 29, 30] were kept fixed, and are presented in Table 1. Since the interaction coefficients for Np(IV) and U(IV) are similar [9], and they have also similar hydration behavior [22, 31], we adopted in the simulation the U(IV)'s LJ parameters for Np(IV).

All calculations at DFT level were performed with the TURBOMOLE v6.3 program package [32] with the BP86 [33–35] exchange-correlation functional due to its good unscaled frequencies [36] and computational performance compared to hybrid functionals. The m5 grid quadrature was employed for the numerical XC term, and entropy calculations were carried out for $T = 198.15$ K and $p = 0.1$ MPa. All molecular structures were optimized without any constraints, and

Table 1 Intermolecular parameters for Lennard-Jones (LJ) intermolecular potential used in Monte Carlo (MC) simulation for water molecules and ions Th⁴⁺ and Np⁴⁺

Specie	Atoms	q_I	ϵ_I	σ_I
H ₂ O	O	-0.8476 ^a	-0.8476 ^a	3.165 ^a
	H	0.4238 ^a	0.000	0.000
	H	0.4238 ^a	0.000	0.000
Th ⁴⁺	Th	+4 ^b	0.080 ^b	2.000 ^b
Np ⁴⁺	Np	+4 ^c	0.17392181 ^c	3.500 ^c

^a From Berendsen, Grigera and Straatsma [29]

^b From Yang, Tsushima and Suzuki [20]

^c From Li, Song and Mertz Jr [30]

frequency calculations were performed numerically to ensure that structures were local minima and to obtain thermochemical corrections. For Th and Np, the small core scalar relativistic ecp-60-mwb pseudo potentials and their corresponding ecp-60-mwb-gencont basis set were employed [37–39], whereas for O and H, the def-TZVP [40] basis set was used. The spin-orbit (SO) effects were neglected in all calculations as recent studies showed SO to be negligible [41, 42], and all binding energies were corrected by counterpoise scheme [43] although the BSSE of these systems were reported as small [23, 44].

The atomic radii employed at COSMO PCM calculations for thorium (IV) [45] and neptunium (IV) [46] were 114 and 128 pm, respectively. For O and H, the recommended values [47, 48] of r of 172 and 130 pm were used.

It is known that dielectric continuum models alone will not give accurate predictions of solvation free energies of charged species due to strong solute–solvent interactions [49, 50]. In order to overcome this limitation, part of the solvent was treated explicitly by the thermodynamic cluster cycle [51–53] depicted in Fig. 1. In this cluster cycle, a cluster of n water molecules reacts with the ionic solute.

The quantum chemical calculations for hydration (solvation) also followed the strategy proposed by Wiebke et al [44], and is presented in Fig. 2. First, gas phase molecular optimizations, frequency and gas phase binding energies D_0 of $[M^{IV}(H_2O)_h]^{4+}$ considering $h = 9$ and 10, and $M = Th$ and Np were performed from geometries obtained from the MC step.

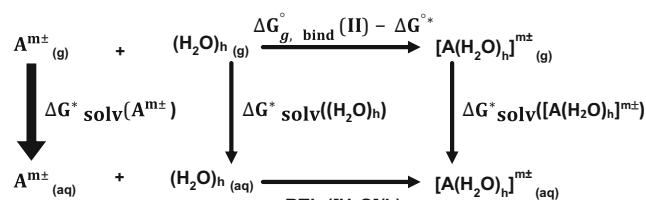
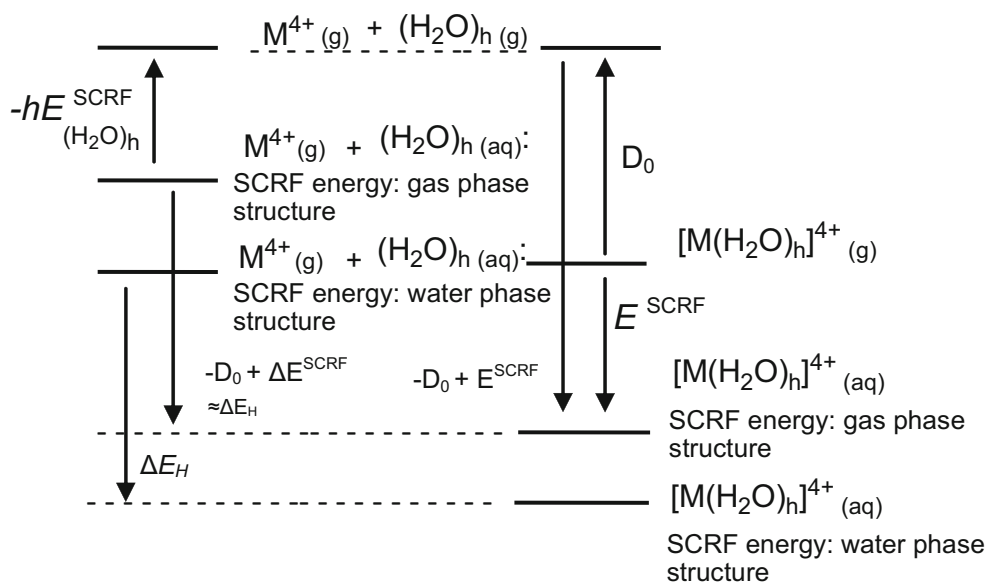


Fig. 1 Thermodynamic cluster cycle for the calculation of $\Delta G_{\text{Sol}}(A^{m\pm})$

Fig. 2 Computational strategy to obtain the Gibbs free energy on hydration for Th⁴⁺ and Np⁴⁺ (adapted from [44])



Hydration energies ΔE_H and Gibbs free energies of hydration were approximated by single-point energies for constrained gas phase structures within COSMO [54] self-consistent reaction field (SCRF).

Equation 1 [55] (see also the thermodynamic cycle in Fig. 3),

$$\Delta\Delta G^*_{x,\text{hydrat, aq}} = \Delta G^0_{x,\text{hydrat, g}} + \Delta\Delta G^*_{\text{solv}} + \Delta G^{0 \rightarrow *}$$
 (1)

where

$$\begin{aligned} \Delta\Delta G^*_{\text{solv}} = & \Delta G^*_{\text{solv}} \left([\text{M}(\text{OH})(\text{H}_2\text{O})_h]^{3+} \right) \\ & + \Delta G^*_{\text{solv}}(\text{H}^+) - \Delta G^*_{\text{solv}} \left([\text{M}(\text{H}_2\text{O})_h]^{4+} \right) \end{aligned}$$
 (2)

, used to obtain the hydrolysis constants, represents how the free energy of the xth reaction step, ΔΔG^{*}_{x,hydrat, aq}, can be written as the sum of the gas phase deprotonation energy (ΔG⁰_{x,hydrat,g}), the differential solvation free energy (ΔΔG^{*}_{solv}) and the standard state correction [55, 56] term (ΔG⁰_{→*}), where the ΔG⁰_{→*} value for 9-fold coordination [57] is -12.43 kJ mol⁻¹.

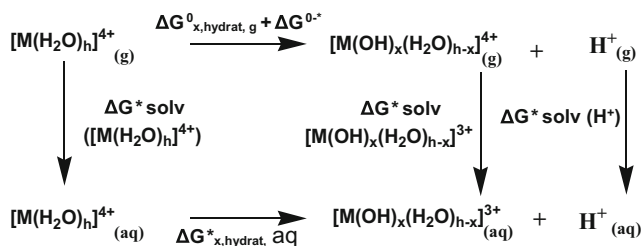
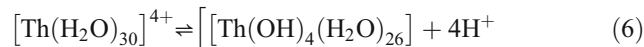
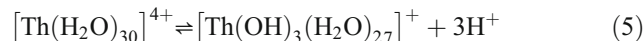
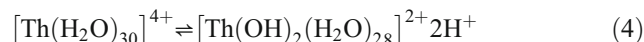


Fig. 3 Thermodynamic cycle used for calculation of Log(K) for Th⁴⁺ hydrolysis

Since the Gibbs free energy for the hydrolysis reactions [9] for Th(IV),



were calculated using the thermodynamic cycle [55] presented in Fig. 3, so a relevant question about the solvated proton presented in these four reactions shows up. The protons on equations 3–6 are in fact solvated ions, which could be a H₅O₂⁺ (Zundel complex ion [58]), or H₃O⁺. The solvation energies for H₅O₂⁺ and H₃O⁺ differ by 43 kJ mol⁻¹, so we decided to use the experimental value [59] of 265.9 kcal mol⁻¹ for the proton free energy of solvation.

Results and discussion

Initially, we considered primary coordination numbers as 8, 9 and 10 for Np(IV) and 9 and 10 for Th(IV) based on results obtained from theoretical studies [19–23]. Since we could not find a structure free of negative frequencies for [Np(OH₂)₈]⁴⁺, we focused the first hydration shell with CN = 9, 10. Structural data obtained from DFT minimizations that gave best concordance to experimental data are presented in Table 2. The inclusion of water dielectric through COSMO lowers the average BP86/ecp-60mwb/def-TZVP bond lengths from 2.54 to 2.47 Å for Th(IV), and from 2.47 to 2.39 Å for Np(IV). Both results in the first solvation shell for <rm-O> average distances are within 0.01 Å compared to experimental data, and

Table 2 Average BP86/ecp-60mwb/def-TZVP $\langle r_{\text{m-O}} \rangle$ bond lengths (in Å) for $[\text{Th}(\text{H}_2\text{O})_9]^{4+}$ and $[\text{Th}(\text{OH})(\text{H}_2\text{O})_8]^{3+}$ in comparison with experimental values

Complex	$\langle r_{\text{m-O}} \rangle$	BP86/ ecp-60mwb def-TZVP (gas phase)	BP86/ ecp-60mwb def-TZVP (COSMO)	Experimental
$[\text{Th}(\text{H}_2\text{O})_9]^{4+}$	Th-O	2.54	2.47	$2.46 \pm 0.02^{\text{a}}$
$[\text{Np}(\text{H}_2\text{O})_9]^{4+}$	Np-O	2.47	2.39	$2.40 \pm 0.01^{\text{b}}$

^a From Moll et al. [14], and Neck and Kim [9]^b From Neck and Kim [9]

also within the experimental error. This seems to indicate a preference for a 9 coordinate environment for both Np(IV) and Th(IV). Our findings are in agreement with experimental [60] and previous theoretical results from Tsushima and Yang [61], but are in contrast with the conclusions drawn by Clark and co-workers [23], who found a thermodynamic preference for the 8-coordination species.

The (negative) zero point energy (ZPE)-corrected gas phase dissociation energies for reaction $[\text{M}(\text{OH}_2)_{\text{h}(\text{g})}]^{4+} \rightarrow \text{M}_{(\text{g})}^{4+} + (\text{OH}_2)_{\text{h}(\text{g})}$ (see also Fig. 4a) were calculated according to the thermodynamic cycle of Fig. 1, and the computational scheme of Fig. 2. As expected, the dissociation energies are of the same order of magnitude of corresponding values [44, 57] for actinide(III), and more negative (Table 3). The dissociation energy shows a smooth increase when one moves from Th(IV) to Np(IV): for $h = 9$, the D_0 increases by $239.48 \text{ kJ mol}^{-1}$ while for $h = 10$ the increase is $246.59 \text{ kJ mol}^{-1}$. The D_0 difference for Th(IV) when the CN increases from 9 to 10 increases by 132 kJ mol^{-1} , while the corresponding value for Np(IV) increases by $139.77 \text{ kJ mol}^{-1}$. The solvent contribution ΔE^{SCRF} increases almost by one order of magnitude less when one moves from Th(IV) to Np(IV) with values for $h = 9$ and 10 of $27.24 \text{ kJ mol}^{-1}$ and $17.15 \text{ kJ mol}^{-1}$, respectively. The interesting point is that the ΔE^{SCRF} decreases as one moves from $h = 9$ to $h = 10$ for Th(IV) by 2.38 kJ mol^{-1} , and the corresponding value for Np(IV) also decreases by $12.47 \text{ kJ mol}^{-1}$. So, the major contribution for free energy of solvation should come from the binding energy.

Now it seems convenient to make some comments about the limitations of the cluster continuum model: within this model, it is possible to include incorrect orientations of water molecules near the dielectric boundary, as well imprecise evaluation of entropic effects of hydrogen bounded complexes. These problems were minimized in this work by including the first (and second solvation shells for the calculation of hydrolysis constants) by MC methods, and by using hydrogen-bonded complexes of similar size in both sides of the thermodynamic cycle [51], respectively.

The calculated Gibbs free energies of solvation are listed in Table 4. The values were calculated according to equations,

$$\Delta G_{\text{Solv}}^0 = \Delta H_{\text{H}}^0 - T\Delta S_{\text{H}}^0 \approx \Delta E_{\text{H}} - T\Delta S^0 \quad (7)$$

and

$$\Delta E_{\text{H}} \approx -D_0 + E^{\text{SCRF}}([A(\text{H}_2\text{O})_h]^{4+}) - E^{\text{SCRF}}((\text{H}_2\text{O})_h). \quad (8)$$

We had to approximate ΔH by ΔE since $\text{An}_{(\text{g})}^{4+}\text{H}^0$ data is neither available from experiment or could not be obtained from quantum chemical calculations. The ΔG^0_{Solv} show better accordance for $h = 9$ when compared to experimental data [62–64]. Since ΔG^0_{Solv} decreases with CN, we also would expect that a Np(IV)'s hypothetical value for $h = 8$ —we could not find a structure free of small negative frequencies for $h = 8$ —would be close to that reported by Clark et al. [23]. The differences at CN = 9 are lower than 1%: they are 24 and

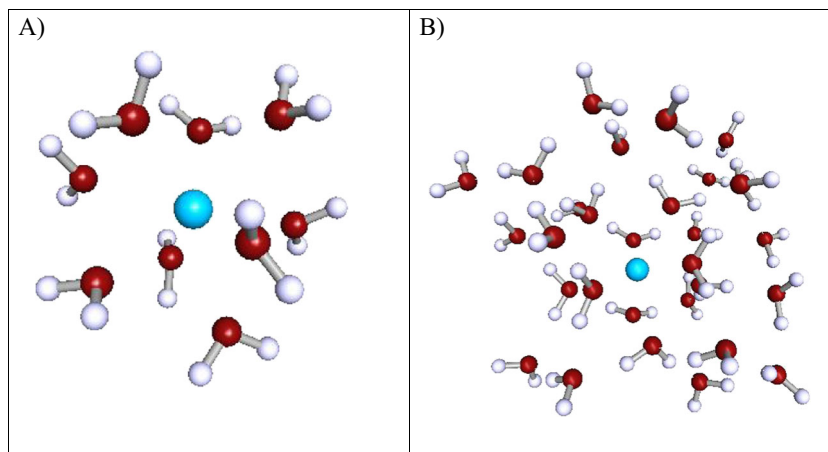
Fig. 4 Representative BP86/ecp-60mwb/def-TZVP optimized geometries for the 1st and 2nd solvation shell structures **a** $[\text{M}(\text{H}_2\text{O})_9]^{4+}$ ($\text{M} = \text{Th}$ or Np) and **b** $[\text{Th}(\text{H}_2\text{O})_{30}]^{4+}$ 

Table 3 Zero point energy (ZPE)-corrected negative gas phase binding energies ($-D_0$) and differences in self-consistent reaction field (SCRF) stabilization energies ΔE^{SCRF} between $[\text{A}(\text{H}_2\text{O})_h]^{4+}$ and $(\text{H}_2\text{O})_h$ (in kJ mol^{-1})

Ion	$-D_0$		ΔE^{SCRF}	
	$h = 9$	$h = 10$	$h = 9$	$h = 10$
Th^{4+}	-3098.81	-3231.47	-2629.22	-2526.84
Np^{4+}	-3338.29	-3478.06	-2656.46	-2543.99

58 kJ mol^{-1} for Th(IV) and Np(IV), respectively. Regarding the question about the coordination numbers: from Tables 2 and 4, the value for both Th(IV) and Np(IV) that is both reasonable and consistent vis-à-vis experimental results is 9.

The hydrolysis constants for Th(IV) are difficult to determine experimentally since they vary with the ionic strength (I), and also because several species appear even at low pH, resulting in complex interconnected equilibria [9]. In general, these constants are obtained [65] in a semi-empirical way and extrapolated to $I = 0$. On the other hand, accurate theoretical equilibrium constants are also a *tour de force* to be obtained, since a change of only $\sim 5 \text{ kJ mol}^{-1}$ (approximately $1.2 \text{ kcal mol}^{-1}$) in ΔG changes $\log K$ by a unit. So it is sensible to expect that an error of 2–3 logarithm units is a very good result due to all the approximations involved in the calculations.

The calculated hydrolysis constants are presented in Table 5, as well corresponding experimental [10, 66–69] available data for $I = 0$. The calculations followed the thermodynamic cycle presented in Fig. 3 (see also Fig. 4b), and results show very good agreement, except for reaction 4, where the constant deviates 3 logarithm units. In addition to the complex equilibria, the hydrolysis constants are also dependent from temperature, concentration and counter ions presented in solution [9]. Concerning the theoretical calculations, even the third solvation shell could be important. Probably, the deviation can be credited mainly to the formation of polymeric species [8], but more research should be done in order to obtain a satisfactory explanation.

Finally, this methodology uses only a GGA functional in all first principles calculations. This opens the perspective to

Table 4 Calculated ΔG_{Solv}^0 (in kJ mol^{-1}) for Th^{4+} e Np^{4+} with different CN numbers (h)

Ion	ΔG_{Solv}^0 (theoretical, this work)		ΔG_{Solv}^0 (theoretical)	ΔG_{Solv}^0 (experimental)
	$h = 9$	$h = 10$		
Th^{4+}	-5836	-5873	-6100 ^a	-5860 ^c
Np^{4+}	-6108	-6133	-6494 ^a , 6069 ^b	-6050 ^c

^a From David and Vokhmin [46]

^b From Clark et al. [23], with $h = 8$

^c From Bratsch and Lagowski [62], Marcus and Loewenschuss [63], and Chopin and Jensen [64]

Table 5 Calculated hydrolysis constants ($\log K$) for $[\text{Th}(\text{H}_2\text{O})_{30}]^{4+}$ reactions for formation of hydroxide complexes using reactions 3–6 (see text for details) at 298.15 K in comparison to experimental data with $I = 0$

Reaction number	Log K (BP/def-TZVP)	Log K (experimental)
3	-2.62	-2.3 ± 0.1^a
		-2.1 ± 0.2^b
		-3.0 ± 0.2^c
4	-9.89	-3.1 ± 0.3^d
		-5.8 ± 0.2^c
		-6.6 ± 0.2^b
5	-8.30	-9.3 ± 0.4^d
		-11.4^b
6	-17.26	-15.9 ± 0.3^c
		-13.6 ± 0.4^d
		-17.0 ± 0.5^b

^a From Brown, Ellis and Sylva [66]

^b From Ekberg et al. [10]

^c From Baes and Mesmer, and Baes; Meyer; Roberts [67, 68]

^d From Grenthe and Lagermann [69]

use RI techniques [70] to include a third hydration shell to obtain better hydrolysis constants, or to include polymeric species and formation of colloidal nanoparticles with actinide (IV) systems. The errors associated to RI are usually small [71], and could be minimized by error cancellation when one performs the energy differences into the thermodynamic cycles, and further investigation is ongoing in this direction.

Conclusions

The study of basic thermodynamic properties is important to reproduce experimental data, and to produce reliable predictions as well. In this study, we investigated gas phase and condensed phase structures, binding energies, hydrolysis constants, structural parameters, and Gibbs free energies for Th(IV) and Np(IV) at $[\text{M}(\text{OH}_2)_h]^{4+}$ with values of $h = 8$ (Np), and 9, 10 (Th and Np) or 30 (Th) using mixed cluster continuum model at BP86/ecp-60mwb/def-TZVP level of theory with starting geometries generated through MC

methods. Our results suggest that, for both ions, the CN should be 9, and for solvation Gibbs free energy the first hydration shell is sufficient. There is very good agreement with available experimental structural data and Gibbs free energy of solvation. There is also good agreement regarding hydrolysis constants at $I = 0$.

Finally, this methodology opens a perspective to use RI techniques for future calculations with a third hydration shell, or to include polymeric species and formation of colloidal nanoparticles with actinide (IV) systems.

Acknowledgments L.G.M.M. acknowledges CNPq (Conselho Nacional de Desenvolvimento Científico e Tecnológico, Brazilian Agency) for his postdoctoral scholarship (Grant number 157843/2015-7). The authors thank FINATEC (Fundação de Empreendimentos Científicos e Tecnológicos) and FAPDF (Fundação de Apoio à Pesquisa do Distrito Federal) for financial support. J. R. Sambrano also thanks Fundação de Amparo à Pesquisa do Estado de São Paulo - FAPESP (Grant numbers 2013/19713-7, 2013/07296-2, 2016/07954-8, 2016/07476-9). The computational facilities were supported by resources supplied by Molecular Simulations Laboratory, São Paulo State University, Bauru, Brazil.

References

- Walter C, Denecke MA (2013) Actinide colloids and particles of environmental concern. *Chem Rev* 113:995–1015
- Brook BW, Bradshaw CJA (2014) Key role for nuclear energy in global biodiversity conservation. *Conserv Biology* 29:702–712
- Cotton S (2006) Lanthanide and actinide chemistry. Wiley, London
- Moulin C, Amekraz B, Hubert S, Moulin V (2001) Study of thorium hydrolysis species by electrospray-ionization mass spectrometry. *Anal Chim Acta* 441:269–279
- Gorden AEV, McKee ML (2016) Computational study of reduction potentials of Th^{4+} compounds and hydrolysis of $\text{ThO}(\text{H}_2\text{O})_n$, $n = 1, 2, 4$. *J Phys Chem A* 120:8169–8183
- Kaszuba JP, Runde WH (1999) The aqueous geochemistry of neptunium: dynamic control of soluble concentrations with applications to nuclear waste disposal. *Environ Sci Technol* 33:4427–4433
- Lombardi C, Luzzi L, Padovani E, Vetrano F (2008) Thorium and inert matrix fuels for a sustainable nuclear power. *Progr Nucl Energy* 50:944–953
- Zanonato PL, Bernardo PD, Zhang Z, Gong Y, Tian G, Gibson JK, Rao L (2016) Hydrolysis of thorium(IV) at variable temperatures. *Dalton Trans* 45:12763–12771
- Neck V, Kim JI (2001) Solubility and hydrolysis of tetravalent actinides. *Radiochim Acta* 89:1–16
- Ekberg C, Albinsson Y, Comarmond MJ, Brown PL (2000) Studies on the complexation behavior of thorium(IV) 1. Hydrolysis Equilibria. *J Sol Chem* 29:63–86
- Antonio MR, Soderholm L, Williams CW, Blaudeau JP, Bursten BE (2001) Neptunium redox speciation. *Radiochim Acta* 89:17–25
- Efurd DW, Runde W, Banar JC, Janecky DR, Kaszuba JP, Palmer PD, Roensch FR, Tait CD (1998) Neptunium and plutonium solubilities in a Yucca Mountain groundwater. *Environ Sci Tech* 32:3893–3900
- Johansson G, Magini M, Ohtaki H (1991) Coordination around thorium (IV) in aqueous perchlorate, chloride and nitrate solutions. *J Sol Chem* 20:775–792
- Moll H, Denecke MA, Jalilehvard F, Sandstrom M, Grenthe I (1999) Structure of the aqua ions and fluoride complexes of uranium (IV) and thorium (IV) in aqueous solution an EXAFS study. *Inorg Chem* 38:1795–1799
- Sandstrom M, Persson I, Jalilehvard F, Lindquist-Reis P, Apangberg D, Hermasson K (2001) Hydration of some large and highly charged ions. *J Synchrotron Rad* 8:657–659
- Rothe J, Denecke MA, Neck V, Muller R, Kim JI (2002) XAFS investigation of the structure of aqueous thorium(IV) species, colloids, and solid thorium (IV) oxide/hydroxide. *Inorg Chem* 41:249–258
- Allen PG, Bucher JJ, Shuh DK, Edelstein NM, Reich T (1997) Investigation of aquo and chloro complexes of UO_2^{2+} , NpO_2^{2+} , Np^{4+} and Pu^{3+} by X-ray absorption fine structure spectroscopy. *Inorg Chem* 36:4676–4683
- Reich T, Bernhard G, Geipel G, Funke H, Hennig C, Rossberg A, Watz W, Schell N, Nitsche H (2000) The Rossendorf beam line ROBL—a dedicated experimental station for XAFS measurements of actinides and other radionuclides. *Radiochim Acta* 88:633–637
- Real F, Trumm M, Vallet V, Schimmelpfennig B, Masella M, Flament JP (2010) Quantum chemical and molecular dynamics study on the coordination of Th(IV) in aqueous solvent. *J Phys Chem B* 114:15913–15924
- Yang T, Tsushima S, Suzuki A (2001) Quantum mechanical and molecular dynamical simulations on Thorium (IV) hydrates in aqueous solution. *J Phys Chem A* 105:10439–10445
- Tsushima S, Yang T, Mochizuki Y, Okamoto Y (2003) Ab initio study on structures of Th(IV) hydrate and its hydrolysis products in aqueous solution. *Chem Phys Lett* 375:204–212
- Tsushima S, Yang T (2005) Relativistic density functional theory study on the structure and bonding of U(IV) and Np(IV) hydrates. *Chem Phys Lett* 401:68–71
- Clark AE, Samuels A, Wisuri K, Landstrom S, Saul T (2015) Sensitivity of solvation environment to oxidation state and position in the early actinide period. *Inorg Chem* 54:6215–6225
- Wang D, van Gunsteren WF, Chai Z (2012) Recent advances in computational actinoid chemistry. *Chem Soc Rev* 41:5836–5865
- Bühl M, Wipff G (2011) Insights into uranyl chemistry from molecular dynamics simulations. *ChemPhysChem* 12:3095–3105
- Vallet V, Macak P, Wahlgren U (2006) Actinide chemistry in solution, quantum chemical methods and models. *Theor Chem Acc* 115:145–160
- Allen MP, Tildesley DJ (1987) Computer simulation of liquids. Clarendon, Oxford
- Coutinho K, Canuto S (2003) DICE: a Monte Carlo program for molecular liquid simulation, University of São Paulo, Brazil, version 2.9
- Berendsen HJC, Grigera JR, Straatsma TP (1987) The missing term in effective pair potentials. *J Phys Chem* 91:6269–6271
- Li P, Song F, Mertz KM Jr (2015) Parametrization of highly charged metal ions using the 12-6-4 LJ type nonbonded model in explicit water. *J Phys Chem B* 119:883–895
- Smirnov PR, Trostin VN (2012) Structural parameters of the nearest surrounding of tri- and tetravalent actinide ions in aqueous solutions of actinide salts. *Russ J Gen Chem* 82:1204–1213
- Ahlrichs R, Bär M, Häser M, Horn H, Kömel C (1989) Electronic structure calculations on workstation computers: the program system TURBOMOLE. *Chem Phys Lett* 162:165–169
- Vosko SH, Wilk L, Nusair M (1980) Accurate spin-dependent electron liquid correlation energies for local spin density calculations: a critical analysis. *Can J Phys* 58:1200–1211
- Becke AD (1988) Density-functional exchange-energy approximation with correct asymptotic behavior. *Phys Rev A* 38:3098–3100
- Perdew JP (1986) Density-functional approximation for the correlation-energy of the inhomogeneous electron gas. *Phys Rev B* 33:8822–8824
- Neugebauer J, Hess BA (2003) Fundamental vibrational frequencies of small polyatomic molecules from density-functional

- calculations and vibrational perturbation theory. *J Chem Phys* 118: 7215–7225
37. Cao X, Dolg M, Stoll H (2003) Valence basis sets for relativistic energy-consistent small-core actinide pseudopotentials. *J Chem Phys* 118:487–496
 38. Cao X, Dolg M (2004) Segmented contraction scheme for small-core actinide pseudopotential basis sets. *J Molec Struct (Theochem)* 673:203–209
 39. Kuechle W, Dolg M, Stoll H, Preuss H (1994) Energy adjusted pseudopotentials for the actinides. Parameter sets and test calculations for thorium and thorium monoxide. *J Chem Phys* 100:7535–7542
 40. Schäfer A, Huber C, Ahlrichs R (1994) Fully optimized contracted gaussian basis sets of triple zeta valence quality for atoms Li to Kr. *J Chem Phys* 100:5829–5835
 41. Parmar P, Samuels A, Clark AR (2015) Applications of polarizable continuum models to determine accurate solution-phase thermochemical values across a broad range of cation charge—the case of U (III–VI). *J Chem Theory Comput* 11:55–63
 42. Clavaguera-Sarrio C, Vallet V, Mayssau D, Marsden CJ (2004) Can density functional methods be used for open-shell actinide molecules? Comparison with multiconfigurational spin-orbit studies. *J Chem Phys* 121:5312–5320
 43. Boys SF, Bernardi F (1970) The calculation of small molecular interactions by the differences of separate total energies. Some procedures with reduced errors. *Mol Phys* 19:553–566
 44. Wiebke J, Moritz A, Cao X, Dolg M (2007) Approaching actinide (+III) hydration from first principles. *Phys Chem Chem Phys* 9: 459–465
 45. Marcus Y (1988) Ionic radii in aqueous solutions. *Chem Rev* 88: 1475–1498
 46. David HF, Vokhmin V (2003) Thermodynamic properties of some tri- and tetravalent actinide aquo ions. *New J Chem* 27:1627–1632
 47. Klamt A, Jonas V, Bürger T, Lohrenz JCW (1998) Refinement and parametrization of COSMO-RS. *J Phys Chem A* 102:5074–5085
 48. Klamt A, Eckert F (2000) COSMO-RS: a novel and efficient method for the a priori prediction of thermophysical data of liquids. *Fluid Phase Equilib* 172:43–72
 49. Chipman CM, Chen F (2006) Cation electric field is related to hydration energy. *J Chem Phys* 124:144507-1–144507-5
 50. Camaioni DM, Dupuis M, Bentley J (2003) Theoretical characterization of oxoanion, XO_m^{n-} , solvation. *J Phys Chem A* 107:5778–5788
 51. Bryantsev VS, Diallo MS, Goddard WA III (2008) Calculation of solvation free energies of charged solutes using mixed cluster/continuum models. *J Phys Chem B* 112:9709–9719
 52. Zhan C-G, Dixon DA (2004) Hydration of the fluorine anion: structures and absolute hydration free energy from first principles electronic structure calculations. *J Phys Chem A* 108:2020–2029
 53. Mejias JA, Lago SJ (2000) Calculation of the absolute hydration enthalpy and free energy of H^+ and OH^- . *J Chem Phys* 113:7306–7316
 54. Klamt A, Schürmann G (1993) COSMO: a new approach to dielectric screening in solvents with explicit expressions for the screening energy and its gradient. *J Chem Soc Perkin Trans* 2:799–805
 55. Bryantsev VS, Diallo MS, Goddard WA III (2009) Computational study of copper(II) complexation and hydrolysis in aqueous solutions using mixed cluster/continuum models. *J Phys Chem A* 113: 9559–9567
 56. Kelly CP, Cramer CJ, Truhlar DG (2006) Aqueous solvation free energies of ions and ion-water clusters based on an accurate value for the absolute aqueous solvation free energy of the proton. *J Phys Chem B* 110:16066–16081
 57. Heinz N, Zhang J, Dolg M (2014) Actinoid III hydration—first principle Gibbs energies of hydration using high level correlation methods. *J Chem Theor Comput* 10:5593–5598
 58. Asthagari D, Pratt LR, Kress JD (2005) Ab initio molecular dynamics and quasichemical study of H^+ . *Proc Natl Acad Sci USA* 102: 6704–6708
 59. Camaioni DM, Schwerdtfeger CA (2005) Comment on “Accurate experimental values for the free energies of hydration of H^+ , OH^- , and H_3O^+ ”. *J Phys Chem A* 109:10795–10797
 60. Antonio R, Soderholm L, Williams CW, Blaudeau JP, Bursten BE (2001) Neptunium redox speciation. *Radiochim Acta* 89:17–25
 61. Tsushima S, Yang T (2005) Relativistic density functional theory on the structure and bonding of U(IV) and Np(IV) hydrates. *Chem Phys Lett* 401:68–71
 62. Bratsch SG, Lagowski JJ (1986) Actinide thermodynamic predictions. 3. Thermodynamics of compounds and aquo-ions of the 2+, 3+, and 4+ oxidation states and standard electrode potentials at 298, 15 K. *J Phys Chem* 90:307–312
 63. Marcus Y, Loewenschuss A (1986) Standard thermodynamic functions of the gaseous actinyl ions $MO_n + 2$ and for their hydration. *J Chem Soc Faraday Trans* 82:2873–2886
 64. Chopin GR, Jensen MP (2010) Actinides in solution: complexation and kinetics. In: Morss LR, Edelstein NM, Fuger J (eds) *The chemistry of the actinide and transactinide elements*, 4th edn, Chapter 23, Springer, Dordrecht, pp 2524–2621
 65. Rossotti FJC, Rossotti H (1961) *The determination of stability constants and other equilibrium constants in solution*, McGraw-Hill, London
 66. Brown PL, Ellis J, Sylva RN (1983) The hydrolysis of metal ions. Part 5. Thorium (IV). *J Chem Soc Dalton Trans* 1983:31–34
 67. Baes CF, Meyer NJ, Roberts CE (1965) The hydrolysis of thorium (IV) at 0 and 95°. *Inorg Chem* 4:518–527
 68. Baes CF, Mesmer RE (1976) *The hydrolysis of cations*. Wiley-Interscience, New York
 69. Grenthe I, Lagermann B (1991) Studies on metal carbonate equilibria. 23. Complex Formation in the Th(IV)- H_2O - $CO_2(g)$ System. *Acta Chem Scand* 45:231–238
 70. Sierka M, Hogeckamp A, Ahlrichs R (2003) Fast evaluation of the coulomb potential for electron densities using multipole accelerated Resolution of Identity approximation. *J Chem Phys* 118:9136–9148
 71. Weingend F, Kattannek M, Ahlrichs R (2009) Approximated electron repulsion integrals: Cholesky decomposition versus resolution of identity methods. *J Chem Phys* 130:164106-1–164106-8